Bioorganic & Medicinal Chemistry 19 (2011) 1115–1122

Contents lists available at ScienceDirect

Bioorganic & Medicinal Chemistry

journal homepage: www.elsevier.com/locate/bmc

Responsive Mn(II) complexes for potential applications in diagnostic Magnetic Resonance Imaging

Gabriele A. Rolla [a], Lorenzo Tei [a], Marianna Fekete [a], Francesca Arena [b], Eliana Gianolio [b], Mauro Botta [a,*]

[a] Dipartimento di Scienze dell'Ambiente e della Vita, Università degli Studi del Piemonte Orientale 'Amedeo Avogadro', Viale T. Michel 11, 15121 Alessandria, Italy
[b] Centre for Molecular Imaging, Dipartimento di Chimica IFM, Università degli Studi di Torino, Via Nizza 52, 10126 Torino, Italy

ARTICLE INFO

Article history:
Received 5 March 2010
Revised 15 July 2010
Accepted 27 July 2010
Available online 2 August 2010

Keywords:
Manganese
Responsive Contrast Agents
Tyrosinase
Molecular Imaging
MRI
Relaxometry

ABSTRACT

The investigation of new Mn(II)-based MRI/Molecular Imaging probes responsive to the enzyme tyrosinase for potential diagnostic applications is herein described. The expression of the enzyme tyrosinase, an oxidoreductase, is up-regulated in melanoma cancer cells. Three novel ligands (**L$_1$**, **L$_2$** and **L$_3$**) were designed as modified acyclic polyaminocarboxylate chelates by introducing an L-tyrosine residue in place of an aminoacetate unit. The corresponding Mn(II) complexes were fully characterised by ^{1}H NMR relaxometric techniques in aqueous media. The responsive activity towards the expression of tyrosinase was then assessed by monitoring the ^{1}H $1/T_1$ relaxivity changes during incubation experiments in buffered solutions containing tyrosinase at different concentrations and in B16F10 melanoma cell homogenate. New insight on the mechanism of action of these systems was gained by measuring the magnetic field dependence of the relaxivity and ESR spectra of the incubated solutions. The systems developed showed responsive activity to tyrosinase with a relaxation enhancement spanning from 50% (Mn**L$_1$**) to 350% (Mn**L$_3$**) which augurs well for the development of diagnostic probes to detect melanoma cancer.

1. Introduction

Over the last three decades Magnetic Resonance Imaging (MRI) has become one of the techniques of choice for diagnostic Imaging. In parallel, the development of efficient contrast enhancing agents (CAs), able to evidence further anatomical details and physiologic information, has yielded very effective tools to access supplementary insight. Currently Gd(III) complexes are by far the MRI CAs most used in clinical practice.[1–4]

However, as Mn^{2+} is a paramagnetic ion with five unpaired electrons (high magnetic moment) and long electronic relaxation time (*S* state electronic structure), high-spin Mn(II) complexes have also attracted interest as potential MRI CAs. In fact, manganese is an essential heavy metal playing a key role as cofactor in a number of important enzymes such as manganese superoxide dismutase and glutamine synthetase.[5,6] A rich biology has evolved to absorb and transport manganese, thus numerous biological structures can complex Mn^{2+} ions with high affinity. Notwithstanding this, only one Mn(II)-based CA, the liver specific Teslascan™ or Mangafodipir™ (Mn-DPDP, DPDP = dipyridoxal diphosphate), is currently approved for clinical practice.[7] Its mode of action is radically different from that of Gd(III)-based CAs: once the complex reaches the liver it slowly releases the metal ion which, after coordination by bio-macromolecules, originates a high MRI signal before being excreted via hepato-biliary route. Although only Mn-DPDP is clinically approved, the search for stable Mn(II)-chelates for possible use as MRI CAs has brought to the synthesis and characterisation of numerous Mn(II) complexes endowed with interesting properties.[8] Another newsworthy application of Mn(II)-based CAs, although only restricted to animal study, is the widely exploited application of $MnCl_2$ MRI, often referred to as MEMRI (Manganese Enhanced Magnetic Resonance Imaging).[9] The scope of this technique comprises the detection of neuronal cell layers in brain structures;[10,11] the study of local brain or cardiac function activity (exploiting Mn(II) as a biological calcium analogue); tracing neuronal projections (exploiting the fact that once inside cells in a specific brain region, Mn(II) will move along appropriate neuronal pathways in an anterograde direction).[12]

A further challenge in the field of MRI CAs is represented by the development of effective protocols for Molecular Imaging, recently defined as 'the visualisation, characterisation and measurement of biological processes at the molecular and cellular levels in humans and other living systems'.[13] A possible approach is the development of probes responsive to specific biochemical events which promote the accumulation of CAs as a consequence of a 'catalytic' action of the target of interest (enzymatic activity,[14–19] pH change,[20] pO_2 change,[21] temperature change[22]). Reporters based on this mode of action can in principle accumulate in large numbers reaching high local concentration and allowing the detection of targets of interest.

* Corresponding author. Tel.: +39 0131360253; fax: +39 0131360250.
E-mail address: mauro.botta@mfn.unipmn.it (M. Botta).

0968-0896/$ - see front matter © 2010 Elsevier Ltd. All rights reserved.
doi:10.1016/j.bmc.2010.07.064

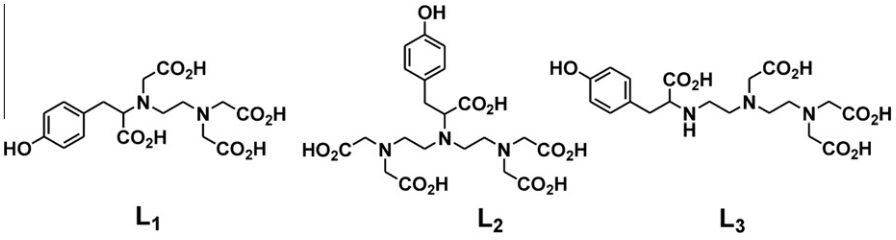

Figure 1. Ligands discussed in this paper.

Prompted by the need of novel Mn(II)-based CAs and willing to address the demand for new Molecular Imaging tools able to probe relevant biochemical events associated with specific pathologies, we designed new Mn(II) complexes, endowed with sufficiently high thermodynamic and kinetic stability, responsive to tyrosinase activity. Tyrosinase is an oxidoreductase over-expressed in melanoma cells which has already been object of considerable interest as a target for developing both imaging probes[18,23] and pro-drug based cancer chemotherapy.[24] The aminoacid L-tyrosine is a natural substrate of tyrosinase which converts it into melanins via a cascade of reactions sketched in Scheme 1.

To probe this approach, we devised simple ligands based on the core structure of H_4EDTA (ethylenediamine-*N*,*N*′-tetraacetic acid), H_5DTPA (diethylenetriamine-*N*,*N*,*N*′,*N*″,*N*″-pentaacetic acid) and H_4DTTA (diethylenetriamine-*N*,*N*,*N*′,*N*″-tetraacetic acid), namely **L_1**, **L_2** and **L_3** (Fig. 1), where an aminocarboxylate unit is substituted with an L-tyrosine residue. We postulated that the coordination sphere of the corresponding Mn(II) complexes could be altered as a consequence of the action of tyrosinase with a concomitant change in relaxivity that can be monitored. In fact, the complex destabilisation would result in a controlled release of metal ion, eventually taken up by biological macromolecules, with an expected, remarkable increase of relaxivity. In fact it is well known that the interaction of Mn^{2+} ions with proteins can give rise to high values of relaxivity.[1] Under this hypothesis, the resulting relaxivity enhancement would arise as a specific consequence of tyrosinase expression for the detection of melanocytes in a possible in vivo application.

2. Results and discussion

2.1. Ligand synthesis

The synthesis of the proposed ligands started with protected L-tyrosine (**1**, Scheme 2), which was monoalkylated with *t*-butyl bromoacetate (Na_2CO_3, MeCN, rt) to give **2**. Following a strategy developed by Rapoport and Williams,[25] **2** was coupled with di-*t*-butyl-2-bromoethyl iminodiacetate (**3**) (Na_2CO_3, MeCN heated under reflux) obtaining the protected ligand **4** in 55% yield after chromatographic purification. Compound **4** was then deprotected (KOH in MeOH–H_2O, rt, followed by TFA, $CHCl_3$, rt) to yield **L_1** as white powder.

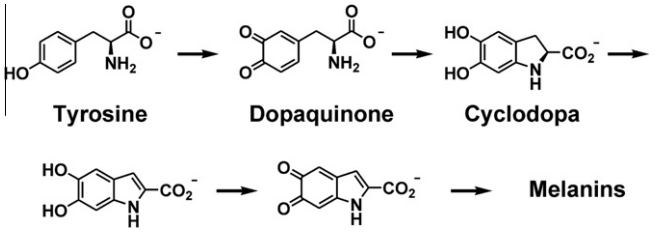

Scheme 1. Biosynthesis of melanines starting from L-tyrosine.

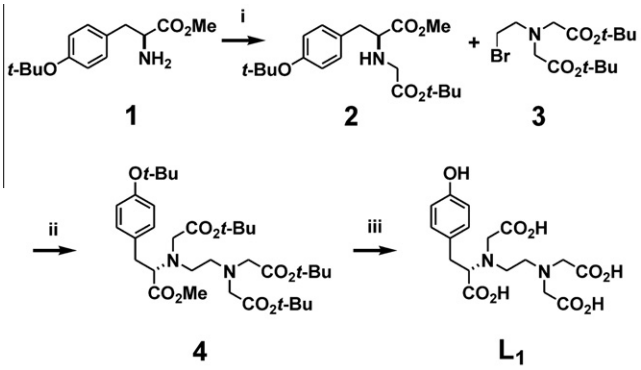

Scheme 2. Reagents and conditions: (i) Na_2CO_3, $BrCH_2CO_2t$-Bu, MeCN, rt, 18 h, 71%; (ii) **3**, Na_2CO_3, MeCN heated under reflux, 48 h, 55%; (iii) (a) KOH in MeOH–H_2O, rt, 4 h; (b) TFA, *i*-Pr_3SiH, $CHCl_3$, rt, 18 h.

In a similar manner, protected L-tyrosine (**5**, Scheme 3) was reacted with three equivalents of **3** (Na_2CO_3, MeCN, under reflux) to give the protected DTPA-like ligand **6**. **L_2** was then obtained by deprotection of **6** under acidic conditions (TFA, $CHCl_3$, rt).

The DTTA-like ligand **L_3** was synthesised starting from *N*-benzyl protected L-tyrosine (**7**, Scheme 4), obtained from **1** by reductive amination with benzaldehyde (PhCHO, $NaBH(OAc)_3$, $C_2H_4Cl_2$, rt). Alkylation with 2-bromoethyltrifluoromethansulfonate[26] (2,6-lutidine, toluene, 0 °C to rt) gave the intermediate **8** which was coupled with tris-*t*-butyl-ethylendiaminotriacetate (**9**)[27] (Na_2CO_3, MeCN heated under reflux) to give the protected ligand **10**. Deprotection of esters and ethers (KOH in MeOH–H_2O, rt; TFA, $CHCl_3$, rt) followed by removal of benzyl protecting group (Pd/C, H_2, MeOH, rt) yielded **L_3** as white solid.

2.2. Complex preparation and relaxometric characterisation

The Mn(II) complexes were prepared by adding to a solution of the ligand (pH 6.5, 298 K) small volumes of a stock solution of

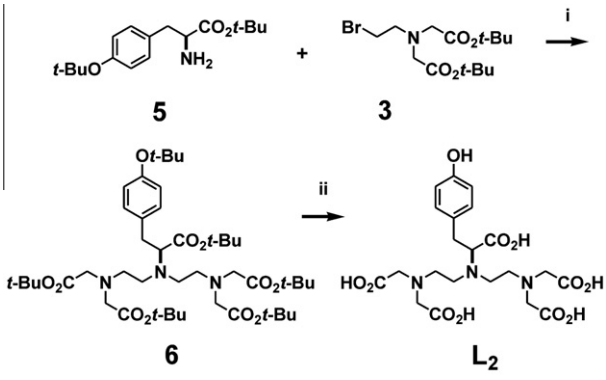

Scheme 3. Reagents and conditions: (i) Na_2CO_3, MeCN, heated under reflux, 48 h, 51%; (ii) TFA, *i*-Pr_3SiH, $CHCl_3$, rt, 18 h.

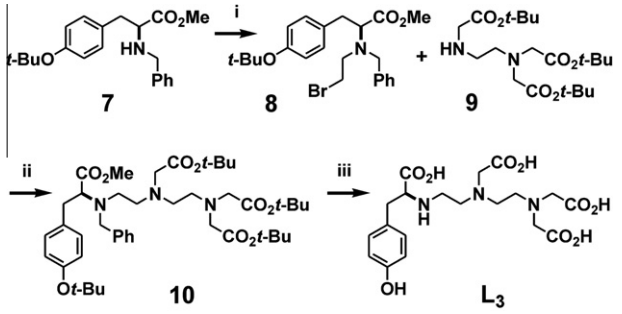

Scheme 4. Reagents and conditions: (i) 2-bromoethyl trifluoromethanesulfonate, 2,6-lutidine, toluene, 0 °C to rt, 48 h, 38%; (ii) Na_2CO_3, MeCN, heated under reflux, 36 h, 32%; (iii) (a) KOH in MeOH–H_2O, rt, 8 h; (b) TFA, $CHCl_3$, rt, 12 h; (c) Pd/C, H_2, MeOH, rt, 18 h.

$Mn(NO_3)_2$ (pH 1.7, 25 °C) and maintaining the pH at 6.5 with diluted NaOH. The complexation process was monitored by measuring the change in the longitudinal water proton relaxation rate (R_1) at 20 MHz as a function of the concentration of Mn(II) added. The straight line obtained has a slope that corresponds to the relaxivity, r_{1p}, of the complex, according to the well known equation:

$$R_1 = r_{1p}[MnL] + R_{1w} \quad (1)$$

where R_{1w} is the diamagnetic contribution and corresponds to 0.38 s^{-1} at 20 MHz and 298 K. The r_{1p} values of the complexes were independently assessed by measuring R_1 and determining the concentration of the solution by mineralisation.[28] These r_{1p} values found are 3.7, 1.7 and 1.6 mM^{-1} s^{-1} for Mn**L**$_1$, Mn**L**$_2$ and Mn**L**$_3$, respectively. The relaxivity of Mn**L**$_1$ is quite similar to that of the parent complex MnEDTA, to indicate that the replacement of an aminocarboxylate with a L-tyrosine did not alter the complexation properties of the ligand. Thus in Mn**L**$_1$ the metal ion is heptacoordinated with one water molecule in its inner coordination sphere (q = 1). The low relaxivity measured for Mn**L**$_2$ and Mn**L**$_3$ may be attributed to the absence of a bound (i.e., inner sphere) water molecule (q = 0) and then to the occurrence of the only outer sphere mechanism of relaxation.[1–4] Also in this case the results reproduce quite closely those found for MnDTPA.[1] The relaxivity of the three complexes was measured also as a function of applied field in the range 0.01–70 MHz at 283, 298 and 310 K, (Fig. 2). These Nuclear Magnetic Relaxation Dispersion (NMRD) profiles were then fitted to the established theory for paramagnetic relaxation and the values of the physico-chemical parameters describing the solute–solvent interaction obtained (Table 1).[1–4] Whereas, the value of most of the parameters is similar for the three complexes and in line with published data for related complexes,[29] the electronic relaxation times for Mn**L**$_2$ appears sensibly longer (shorter Δ^2) than for Mn**L**$_3$, consistent with a higher local symmetry around Mn ion. Finally, the constant value of r_{1p} with pH in the interval 4–12 (20 MHz, 298 K) confirmed the integrity and stability of the complexes with respect to coordination equilibria and/or hydrolytic processes.

2.3. Incubation experiments

Incubation experiments of Mn**L**$_1$, Mn**L**$_2$ and Mn**L**$_3$ with tyrosinase, at 37 °C in buffered conditions (50 mM phosphate, pH 6.5; 5 mM hepes, pH 7.4), were carried out monitoring the variation of R_1 at 20 MHz for dilute solutions of the complex (0.4–1.5 mM) as a function of incubation time (0–20 h). In particular, for each complex three experiments were run by varying the loading of enzyme (50, 250 and 500 U). For all the experiments an increase of the longitudinal water proton relaxation rate was measured and the degree of this effect was expressed with an enhancement coef-

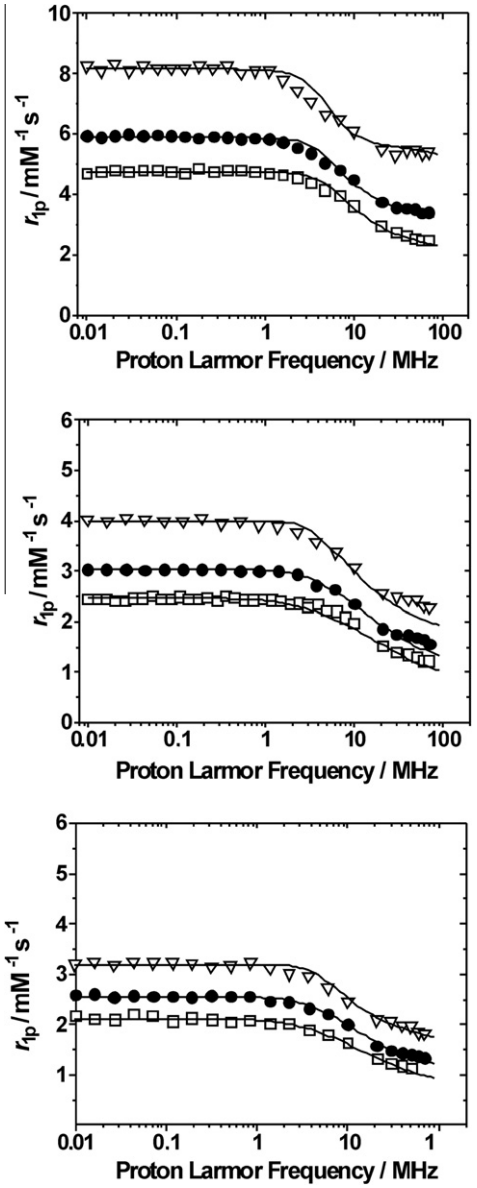

Figure 2. $1/T_1$ ^{1}H NMRD profiles of Mn**L**$_1$ (top), Mn**L**$_2$ (middle) and Mn**L**$_3$ (bottom) at pH 6.5 and at 283 K (open triangles), 298 K (filled circles) and 310 K (open squares).

Table 1
Best-fit parameters obtained from the analysis of the $1/T_1$ NMRD profiles of the Mn-complexes

Parameter	Mn**L**$_1$	Mn**L**$_2$	Mn**L**$_3$
Δ^{2a} (s^{-2} 10^{19})	6.7 ± 0.3	3.8 ± 0.2	6.5 ± 0.2
$^{298}\tau_V{}^a$ (ps)	29.1 ± 1.3	25.5 ± 1.1	22.3 ± 0.7
$^{298}\tau_R$ (ps)	75.4 ± 0.6	/	/
r^b (Å)	2.92	/	/
q^c	1	0	0
a^d (Å)	3.2 ± 0.1	3.2 ± 0.1	3.4 ± 0.1
D^e (cm^2 s^{-1} 10^{-5})	2.24	2.24	2.24

[a] Parameters of the electronic relaxation times: the trace of the square of the zero-field splitting tensor, Δ^2, and the correlation time describing the modulation of the zero-field splitting, τ_V.
[b] Mean Mn–H (water) distance of the coordinated water molecule.
[c] Fixed during the fitting.
[d] Distance of closest approach of the bulk water molecules to the metal ion.
[e] Relative diffusion coefficient of solute and solvent, fixed during the fitting.

ficient, ε^*, defined as the ratio of R_1 after a time t of incubation (R_1^t) over the corresponding initial value of R_1 (R_1^0):

$$\epsilon^* = (R_1^t - R_{1w})/(R_1^0 - R_{1w}) \quad (2)$$

The parameter ε_F^* can be defined as the limiting value of ε^*. The stability of the Mn(II) complexes in the absence of enzyme was proved by incubation under identical conditions of concentration, pH, buffer and temperature to those used in the experiment with the enzyme. No changes in R_1 with time could be measured in the absence of tyrosinase. The incubation experiment of Mn**L**$_1$ was carried out on a 0.4 mM solution in 50 mM phosphate buffer (pH 6.5; 37 °C) and the relaxation rate was measured at 20 MHz at intervals of ca. 10–20 min. A relaxation enhancement is observed that reaches a plateau in about 120/150 min. The largest enhancement corresponds to a relaxivity increase of 51% ($\epsilon_F^* = 1.51$) and is observed using 500 U of enzyme after ca. 3 h of incubation (Fig. 3A).

In order to investigate the mechanism responsible for the observed relaxation enhancement, the $1/T_1$ NMRD profile of the solution containing Mn**L**$_1$ and the enzyme after incubation was measured at 37 °C. As compared with the corresponding profile of the intact complex, the relaxivity after the incubation period is increased over the entire magnetic field range (Fig. 4A). In particular, the relaxivity gain is more pronounced at low frequencies (<ca. 1 MHz) where it is possible to detect a dispersion at ca. 0.3 MHz attributable to the contact term. This result suggests the presence in the incubated solution of Mn(II) aquaion. To check this hypothesis we measured the NMRD profile under identical experimental condition (50 mM phosphate buffer; pH 6.5; 37 °C) of a equimolar solution of $Mn(NO_3)_2$. The shape of this profile is quite similar to that reported in Figure 4A but its amplitude is about 3.6 times larger. From these data we can estimate that part of the initial concentration of Mn**L**$_1$ was converted into the metal aquaion, whereas the remaining part is likely to correspond either to unmodified Mn**L**$_1$ complex or to low-relaxing oligomers that contribute only marginally to the observed NMRD profile. Further evidence of the release of free Mn(II) ions was obtained by measuring ESR spectra on the same mixture. In fact, while Mn(II) aquaion originates a typical ESR multiplet (Fig. 5B-i), the Mn(II) chelates generally do not give rise to an ESR signal in aqueous media at room temperature. Thus, while Mn**L**$_1$ is ESR silent (Fig. 5B-ii), after its incubation with tyrosinase the ESR signal is partially restored (Fig. 5B-iii), suggesting some release of Mn^{2+} ions.

In order to check a possible active role of the strongly coordinating environment associated with 50 mM phosphate buffer in the Mn(II) decomplexation and to better reproduce the physiologic pH conditions, the incubation experiment was repeated in 5 mM hepes buffer at pH 7.4. Surprisingly, the enhancement observed is almost negligible. Probably tyrosinase catalyses the formation of low stability structures from which manganese can be released by strongly coordinating anions such as phosphate. On the other hand, in the presence of the non coordinating hepes buffer the decomplexation of Mn^{2+} ions is markedly reduced.

Analogous incubation experiments were carried out on Mn**L**$_2$ and Mn**L**$_3$ and a good enhancement was observed both in 50 mM phosphate buffer (pH 6.5) and in 5 mM hepes buffer (pH 7.4) (Fig. 3B and C). For both complexes the relaxation enhancements observed are significantly larger than those found for Mn**L**$_1$. The ε_F^* values corresponding to the incubation in the presence of 500 U of tyrosinase are 2.91 and 3.56 for Mn**L**$_2$ and Mn**L**$_3$, respectively. These high values reflect the fact that whereas Mn**L**$_1$ has $q = 1$ and a relaxivity of ca. 2.9 $mM^{-1}\,s^{-1}$ at 37 °C, Mn**L**$_2$ and Mn**L**$_3$ have $q = 0$ and then relaxivity values of only 1.5 and

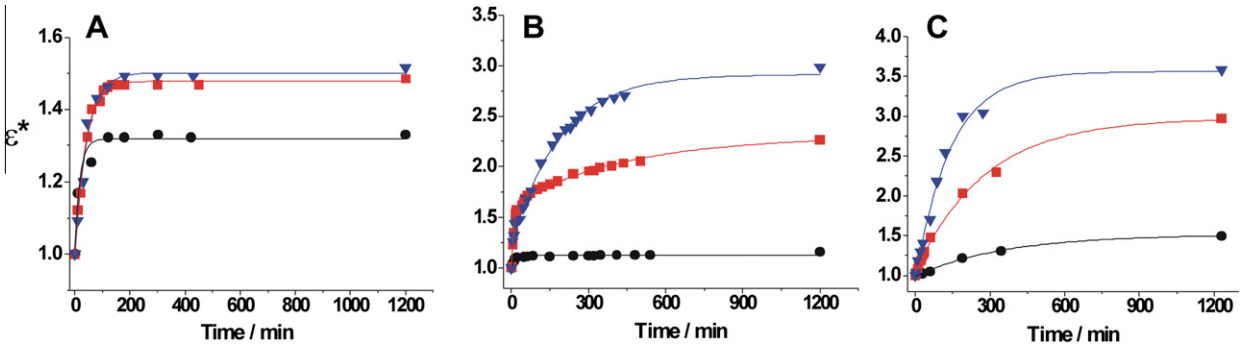

Figure 3. Enhancement factor ε^*, at 20 MHz and 310 K, as a function of incubation time for buffered solutions of Mn**L**$_1$ (A), Mn**L**$_2$ (B) and Mn**L**$_3$ (C) in the presence of different tyrosinase concentration (black circles: 50 U; red squares: 250 U; blue triangles: 500 U).

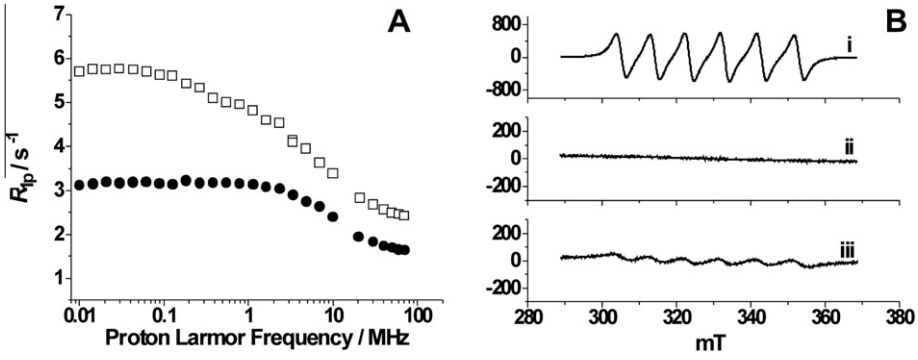

Figure 4. (A) $1/T_1$ ^{1}H NMRD profiles at 310 K and pH 6.5 of a 0.6 mM solution of Mn**L**$_1$ in phosphate buffer after incubation with 500 U of tyrosinase (open squares) and of a 0.6 mM solution of Mn**L**$_1$ in water (filled circles); (B) X-band ESR spectra at 25 °C of: (i) 0.6 mM aqueous solution of $Mn(NO_3)_2$; (ii) 0.6 mM aqueous solution of Mn**L**$_1$ (pH 6.5); (iii) 0.6 mM solution of Mn**L**$_1$ in phosphate buffer (pH 6.5) after incubation at 310 K with 500 U of tyrosinase.

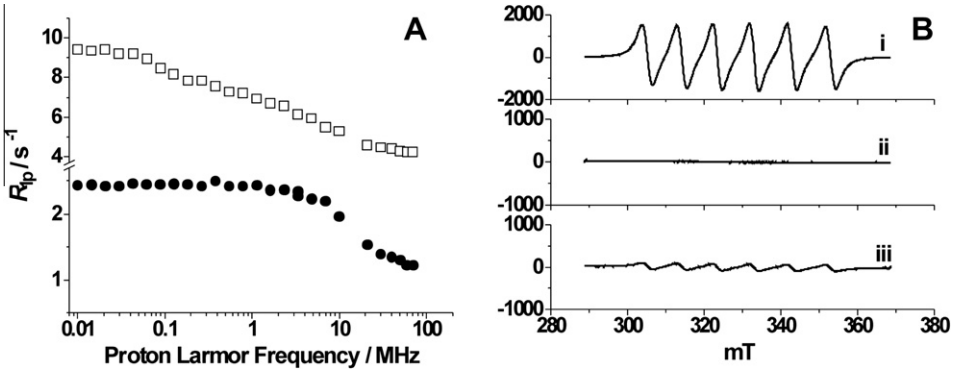

Figure 5. (A) $1/T_1$ ^{1}H NMRD profiles at 310 K and pH 7.4 of a 1.5 mM solution of Mn**L$_2$** in hepes buffer after incubation with 500 U of tyrosinase (open squares) and of a 1.5 mM solution of Mn**L$_2$** in water (filled circles); (B) X-band ESR spectra at 25 °C of: (i) 1.5 mM aqueous solution of $Mn(NO_3)_2$; (ii) 1.5 mM aqueous solution of Mn**L$_2$** (pH 7.4); (iii) 1.5 mM solution of Mn**L$_2$** in hepes buffer (pH 7.4) after incubation at 310 K with 500 U of tyrosinase.

1.3 mM^{-1} s^{-1} at the same temperature. Then, these two complexes combine a higher stability (higher denticity of the ligand) to a lower intrinsic relaxivity that allows for larger enhancement upon enzymatic activity. ^{1}H NMRD profiles and ESR spectra revealed that, whereas for Mn**L$_2$** the enhancement effect seems to be associated with a complex destabilization and release of free Mn^{2+} ion (Fig. 5), for Mn**L$_3$** a different mechanism of enzymatic activity appears to be involved. In fact, the ESR spectrum of the mixture after incubation does not show any presence of free Mn^{2+} ions and the NMRD profile shows a relaxivity peak around 40 MHz which is characteristic of the presence of slowly tumbling oligomeric species (Fig. 6). Polymerisation is an expected reactivity pathway for tyrosinase, as previously exploited for Gd-based tyrosinase and myeloperoxidase responsive agents.[17,18] Remarkably, this pathway was observed only in the case of Mn**L$_3$** and not for Mn**L$_1$** and Mn**L$_2$**. We surmised a correlation of the different reactivity with the presence in Mn**L$_3$** of a secondary amine in the tyrosine residue which might promote a reaction pathway similar to that of melanin biosynthesis (i.e., formation of polyphenolic biopolymers). It is worth noting that, while in the case of Mn**L$_1$** and Mn**L$_2$** the enzymatic activity causes destabilization of the complex, the formation of oligomers observed for Mn**L$_3$** seems not to be associated with destabilization of the monomeric units.

2.4. Incubation experiments on B16 melanoma cell homogenate

In order to evaluate more closely the potential application of the designed Mn(II) complexes to the detection of tyrosinase in vivo, Mn**L$_2$** and Mn**L$_3$** were incubated with B16F10 murine melanoma cell homogenate. B16F10 melanoma cells have been used for the enzymatic assays, as this cell line has been reported to possess high tyrosinase activity related to its natural melanin pigmentation.[30–32]

Cellular tyrosinase activity was assayed according to the method of Tomita et al.[33] using L-DOPA as substrate and following the conversion of DOPA to DOPAchrome via DOPA quinone. B16F10 cells (ca. 1×10^6) were washed with PBS, added to 0.5 mL of a 1 mM L-DOPA solution, sonicated in order to induce cell lysis, and the absorbance at 475 nm was measured over time by maintaining the temperature of the reaction mixture at 310 K (Fig. 7A). The increase of absorbance with time reports about the DOPAchrome formation and so about the cells tyrosinase activity. In these proliferation conditions, the enzymatic activity of one million of cells has been estimated to be ca. 30 U (the extinction coefficient of DOPAchrome at 475 nm is 3700 M^{-1} cm^{-1}).

Then, Mn**L$_2$** and Mn**L$_3$** were tested on B16F10 lysates. B16 cells (ca. 5×10^6) were washed with PBS, added to 100 μL of a 1 mM solution of Mn**L$_2$** or Mn**L$_3$**, sonicated to induce cell lysis and the proton longitudinal relaxation rate at 20 MHz was measured over time by maintaining the temperature of the reaction mixture at 310 K (Fig. 7B). An increase of the observed relaxation rate as a function of time was observed, as previously found for the incubation experiments with the isolated tyrosinase (Fig. 3B and C). The relatively low relaxation enhancements observed in Figure 7B are comparable to those obtained with the lower (50 U) enzyme loading used in the experiments reported in Figure 3B and C. This is

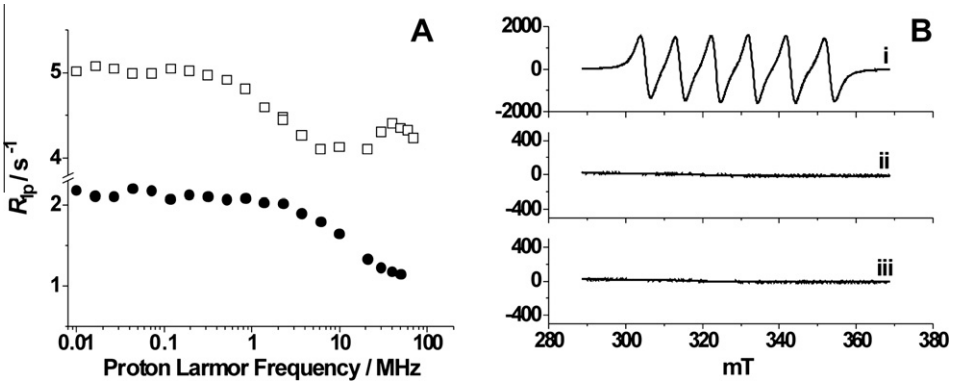

Figure 6. (A) $1/T_1$ ^{1}H NMRD profiles at 310 K and pH 7.4 of a 1.5 mM solution of Mn**L$_3$** in hepes buffer after incubation with 500 U of tyrosinase (open squares) and of a 1.5 mM solution of Mn**L$_3$** in water (filled circles); (B) X-band ESR spectra at 25 °C of: (i) 1.5 mM aqueous solution of $Mn(NO_3)_2$; (ii) 1.5 mM aqueous solution of Mn**L$_3$** (pH 7.4); (iii) 1.5 mM solution of Mn**L$_3$** in hepes buffer (pH 7.4) after incubation at 310 K with 500 U of tyrosinase.

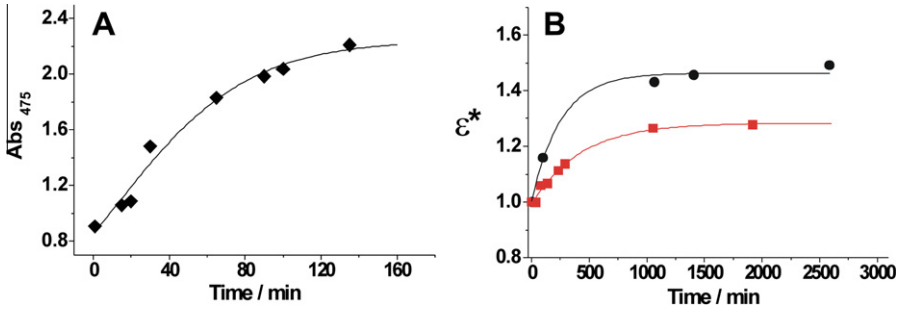

Figure 7. (A) Absorbance at 475 nm as a function of time for B16F10 cells homogenates added to a 0.5 mL of a 1 mM L-DOPA solution; (B) relaxivity enhancement factors as a function of time for solutions of Mn**L**$_2$ (0.74 mM; black circles) and Mn**L**$_3$ (0.56 mM; red squares) incubated in B16F10 homogenates.

consistent with the rather low tyrosinase activity measured on the cells lysates when compared to the experiments carried on in the presence of 250 U and 500 U of tyrosinase.

3. Conclusions

In this study, new Mn(II) complexes responsive to the enzyme tyrosinase were synthesised and their responsive activity was evaluated in vitro both by incubation with isolated tyrosinase and by incubation in B16 cell homogenate. A remarkable relaxation enhancement effect was detected, especially in the experiments with the outer sphere complexes Mn**L**$_2$ and Mn**L**$_3$, confirming the hypothesis initially postulated. In principle it was expected that the different loading of enzyme would effect the rate of change of R_1 but not its limiting value (ε_F^*). The observed dependence of the enhancement factor after 20 h of incubation from the loading of tyrosinase used could be due to a relatively low turnover of the enzyme; therefore, higher loading would allow a larger amount of substrate to be converted by the enzyme, thus giving rise to larger relaxation enhancement effects.

The mechanism of action proposed is based on the destabilisation of Mn(II) complexes followed by release of free Mn^{2+} ion in a similar manner as with MnDPDP, approved for clinical use. NMRD profiles and ESR spectra of the mixtures of Mn(II) complexes and tyrosinase/B16 cell homogenate confirmed release of some free Mn^{2+} ion in the case of Mn**L**$_1$ and Mn**L**$_2$, whereas for Mn**L**$_3$ the formation of oligomeric species seems responsible for the increased relaxivity. As the expression of tyrosinase is associated with melanoma cancer, a method able to detect it in vivo could potentially find application as a diagnostic tool for early diagnosis of melanoma.

4. Experimental

4.1. Materials and instrumentation

All chemicals were purchased from Sigma–Aldrich Co., Alfa Aesar Co. and Bachem Co. and were used without purification unless otherwise stated. Compounds *tert*-butyl 2-bromoethylethyleneaminodiacetate (**3**),[25] 2-bromoethyl trifluoromethanesulfonate[26] and tris-*t*-butyl ethylenediaminotriacetate (**9**)[27] were prepared following previously reported procedures. NMR spectra were recorded on a on a JEOL Eclipse Plus 400 spectrometer operating at 9.4 Tesla. ESI mass spectra were recorded on a Waters SQD 3100. ESR spectra were recorded using a JEOL FA-200 ESR X-band spectrometer with JEOL ES-LC11 flat cell for aqueous samples analysis. ESR spectroscopic analyses were carried out under the following conditions: temperature 298 K; magnetic field 328 ± 40 mT; field modulation width 0.3 mT; field modulation frequency 100 KHz; time constant 0.03 s; sweep time 2 min; microwave frequency 9.226 GHz, microwave power 10 mW. For the measurement of the relaxation rates, the standard inversion-recovery method was employed (16 experiments, 2 scans) with a typical 90° pulse width of 3.5 ms, and the reproducibility of the T_1 data was ±0.5%.

The exact concentrations of manganese were determined by mineralisation of samples in HNO_3 and by measuring their water proton relaxation rates.[28] The temperature was controlled with a Stelar VTC-91 airflow heater equipped with a calibrated copper–constantan thermocouple (uncertainty of ±0.1 °C). The proton $1/T_1$ NMRD profiles were measured on a fast field-cycling Stelar SmarTracer relaxometer over a continuum of magnetic field strengths from 0.00024 to 0.25 T (corresponding to 0.01–10 MHz proton Larmor frequencies). The relaxometer operates under computer control with an absolute uncertainty in $1/T_1$ of ±1%. Additional data points in the range 15–70 MHz were obtained on the Stelar Spinmaster spectrometer.

4.2. Synthesis of ligands

4.2.1. Methyl (2*S*)-2-(*tert*-butoxycarbonylmethyl-amino)-3-(4-*tert*-butoxy-phenyl)-propionate (2)

Neat *tert*-butyl bromoacetate (487 μL; 3.30 mmol) was added drop-wise over 2 min into a suspension of Na_2CO_3 (1.10 g; 10.4 mmol) and L-Tyr(O*t*Bu)-OMe (**1**) (1.00 g; 3,47 mmol) in MeCN (10 mL). After being vigorously stirred 18 h at rt the mixture was centrifuged; the solid was washed with EtOAc (3 × 15 mL) and the solution was concentrated and purified by column chromatography (petroleum ether/EtOAc 5:1–3:1) to give a colourless oil (900 mg; 71%). ^{1}H NMR ($CDCl_3$) 400 MHz: δ = 1.28 (s, 9H, *t*-Bu), 1.39 (s, 9H, *t*-Bu), 2.91 (d, 2H, J = 7.0 Hz, $ArCH_2$), 3.18 (d, 1H, J = 17.0 Hz , $CHCO_2t$-Bu), 3.26 (d, 1H, J = 17.0 Hz , $CHCO_2t$-Bu), 3.50 (t, 1H, J = 7.0 Hz, $CHCO_2Me$), 3.57 (s, 3H, CO_2Me), 6.86 (d, 2H, J = 8.4 Hz, Ar), 7.04 (d, 2H, J = 8.4 Hz, Ar) ppm. ^{13}C NMR ($CDCl_3$) 100 MHz: δ = 28.0 (CH_3, *t*-Bu), 28.8 (CH_3, *t*-Bu), 38.9 (CH_2, $ArCH_2$), 49.9 (CH_2), 51.6 (CH_3, CO_2Me), 62.3 (CH, $CHCO_2Me$), 78.2 (C, *t*-Bu), 81.2 (C, *t*-Bu), 124.1 (CH, Ar), 129.6 (CH, Ar), 131.7 (C, Ar), 154.1 (C, Ar), 170.6 (C, CO), 174.1 (C, CO) ppm. ESI-MS (*m/z*): 366.3 ($M+H^+$); 388.3 ($M+Na^+$).

4.2.2. Methyl (2*S*)-2-((2-(bis-*tert*-butoxycarbonylmethyl-amino)-ethyl)-*tert*-butoxycarbonylmethyl-amino)-3-(4-*tert*-butoxy-phenyl)-propionate (4)

A suspension of **2** (900 mg; 2.46 mmol), *tert*-butyl 2-bromoethyl iminodiacetate (**3**) (1.73 g; 4.93 mmol) and Na_2CO_3 (783 mg, 3.78 mmol) in MeCN (9 mL) was heated under reflux. After 24 h, more **3** (200 mg) was added and the reaction was continued for further 24 h. Then the reaction mixture was centrifuged and the solid residue was washed with EtOAc (3 × 15 mL). The resulting solution was concentrated and purified by column chromatography (petroleum ether/EtOAc 5:1–3:1) to give a colourless oil (864 mg; 55%). ^{1}H NMR ($CDCl_3$) 400 MHz: δ = 1.29 (s, 9H, *t*-Bu),

1.44 (s, 27 H, CO_2t-Bu), 2.70–2.99 (m, 6H, CH_2), 3.36 (d, 2H, J = 17.7 Hz, 2CH), 3.43 (d, 2H, J = 17.7 Hz, CH_2CO_2t-Bu), 3.50 (s, 2H, CH_2CO_2t-Bu), 3.55 (s, 3H, CO_2Me), 3.75 (t, 1H, J = 8.2 Hz, $CHCO_2Me$), 6.85 (d, 2H, J = 8.2 Hz, Ar), 7.09 (d, 2H, J = 8.2 Hz, Ar) ppm. ^{13}C NMR ($CDCl_3$) 100 MHz: δ = 27.8 (CH_3, t-Bu), 28.6 (CH_3, t-Bu), 35.7 (CH_2, $ArCH_2$), 50.5 (CH_2, NCH_2), 50.8 (CH_3, CO_2Me), 52.4, 52.9, 55.7 (CH_2, NCH_2), 65.8 (CH, $CHCO_2Me$), 77.7 (C, t-Bu), 80.2 (C, t-Bu), 80.4 (C, t-Bu), 123.6 (CH, Ar), 129.4 (CH, Ar), 132.6 (C, Ar), 153.4 (C, Ar), 170.3 (C, CO), 170.7 (C, CO), 172.4 (C, CO) ppm. ESI-MS (m/z): 637.5 ($M+H^+$); 659.5 ($M+Na^+$).

4.2.3. (2*S*)-2-((2-(Bis-carboxymethyl-amino)-ethyl)-carboxy methyl-amino)-3-(4-hydroxy-phenyl)-propionic acid (L1)

A solution of **4** (864 mg, 1.36 mmol) and KOH (91 mg, 1.63 mmol), in 1:1 MeOH–H_2O (3 mL) was stirred at rt for 4 h; more KOH (180 mg, 3.21 mmol) was added and the reaction mixture was kept stirring for further 4 h. Then MeOH was removed in vacuo and the mixture was lyophilised after being acidified to pH 2. The resulting solid was triturated under acidic water (pH 2) then suspended in $CHCl_3$ (7 mL) containing i-Pr_3SiH (5 μL) and treated with TFA (2 mL). The reaction mixture was stirred for 18 h and then concentrated in vacuo to give a white solid. ^1H NMR (D_2O + NaOD, pD = 8.5) 400 MHz: δ = 2.86–3.25 (m, 4H, CH_2CH_2), 3.39–3.42 (m, 2H, CH_2), 3.61 (d, 1H, J = 7.0 Hz, CH_2CO_2H), 3.64 (d, 1H, J = 7.0 Hz, CH_2CO_2H), 3.84 (d, 1H, J = 3.3 Hz, $NCHCO_2H$), 3.96 (d, 2H, J = 17.6 Hz, CH_2CO_2H), 4.05 (d, 2H, J = 17.6 Hz, CH_2CO_2H), 6.84 (d, 2H, J = 8.8 Hz, Ar), 7.16 (d, 2H, J = 8.8 Hz, Ar) ppm. ^{13}C NMR (D_2O + NaOD) 100 MHz: δ = 34.5 (CH_2, $ArCH_2$), 49.6, 50.7, 53.3, 54.1 (CH_2, NCH_2), 66.2 (CH, $NCHCO_2H$), 119.5 (CH, Ar), 128.3 (CH, Ar), 130.1 (C, Ar), 157.9 (C, Ar), 171.3 (C, CO), 173.5 (C, CO) ppm. ESI-MS (m/z): 397.3 ($M-H^+$).

4.2.4. *tert*-Butyl (2*S*)-2-(bis-(2-(bis-*tert*-butoxycarbonylmethyl-amino)-ethyl)-amino)-3-(4-*tert*-butoxy-phenyl)-propionate (6)

A suspension of **3** (449 mg, 1.28 mmol), L-Tyr(OtBu)-OtBu (**5**) (150 mg, 0.425 mmol) and Na_2CO_3 (180 mg, 1.7 mmol) in MeCN (3 mL) was heated under reflux for 48 h. The reaction mixture was centrifuged and the solid residue was washed with EtOAc (3 × 10 mL). The resulting solution was concentrated and purified by column chromatography (petroleum ether/EtOAc 5:1–3:1) to give a light-yellow oil (182 mg; 51%). ^1H NMR ($CDCl_3$) 400 MHz: δ = 1.29 (s, 9H, t-Bu), 1.38 (s, 45 H, CO_2t-Bu), 2.63–2.99 (m, 10H), 3.51 (s, 8H, CH_2CO_2t-Bu), 3.57–3.61 (m, 1H, $NCHCO_2t$-Bu), 6.84 (d, 2H, J = 8.2 Hz, Ar), 7.08 (d, 2H, J = 8.2 Hz, Ar) ppm. ^{13}C NMR ($CDCl_3$) 100 MHz: δ = 28.1 (CH_3, t-Bu), 28.8 (CH_3, t-Bu), 35.4 (CH_2, $ArCH_2$), 50.2, 53.3, 53.4, 56.0 (CH_2, NCH_2), 65.7 (CH, $CHCO_2t$-Bu), 78.0 (C, t-Bu), 80.2 (C, t-Bu), 80.7 (C, t-Bu), 123.8 (CH, Ar), 129.7 (CH, Ar), 133.4 (C, Ar), 153.5 (C, Ar), 170.5 (C, CO) ppm. ESI-MS (m/z): 836.6 ($M+H^+$); 858.6 ($M+Na^+$).

4.2.5. (2*S*)-2-(Bis-(2-(bis-carboxymethyl-amino)-ethyl)-amino)-3-(4-hydroxy-phenyl)-propionic acid (L2)

A solution of **6** (182 mg, 0.218 mmol) in $CHCl_3$ (2 mL) containing i-Pr_3SiH (5 μL) and treated with TFA (400 μL). The reaction mixture was stirred for 18 h and then concentrated in vacuo to give a white solid. ^1H NMR (D_2O + NaOD) 400 MHz: δ = 2.45–2.90 (m, 10H), 3.08 (s, 8H), 3.26 (m, 1H), 6.47 (d, 2H, J = 8.4 Hz, Ar), 6.91 (d, 2H, J = 8.4 Hz, Ar) ppm. ^{13}C NMR (D_2O + NaOD, pD = 8.5) 100 MHz: δ = 35.3 (CH_2, $ArCH_2$), 48.9, 53.0, 59.3 (CH_2, NCH_2), 70.3 (CH, $CHCO_2H$), 118.8 (CH, Ar), 124.8 (C, Ar), 130.6 (CH, Ar), 164.6 (C, Ar), 179.8 (C, CO) ppm. ESI-MS (m/z): 498.7 ($M-H^+$).

4.2.6. Methyl (2*S*)-2-benzylamino-3-(4-*tert*-butoxy-phenyl)-propionate (7)

A solution of L-Tyr(OtBu)-OMe (**1**) (1.0 g, 3.47 mmol) and benzaldehyde (360 μL, 3.54 mmol) in anhydrous 1,2-dichloroethane (10 mL) was stirred for 30 min and then $NaBH(OAc)_3$ (736 mg, 3.55 mmol) was added in one portion. After 24 h $NaBH_4$ (70 mg, 1.85 mmol) was added in one portion and the resulting mixture was stirred for additional 20 min before being quenched with a saturated solution of $NaHCO_3$ (5 mL) and extracted in CH_2Cl_2 (3 × 15 mL). The organic layer was dried over Na_2SO_4, concentrated in vacuo and purified by column chromatography (petroleum ether/EtOAc 5:1–3:1) to give a light yellow oil (813 mg, 67%). ^1H NMR ($CDCl_3$) 400 MHz: δ = 1.41 (s, 9H, t-Bu), 3.00 (d, 2H, J = 7.0 Hz, $ArCH_2$), 3.59 (t, 1H, J = 7.0 Hz, $CHCO_2Me$), 3.69 (s, 3H, CO_2Me), 3.71 (d, 1H, J = 13.3 Hz, CHPh), 3.90 (d, 1H, J = 13.3 Hz, CHPh), 6.99 (d, 2H, J = 8.4 Hz, Ar), 7.14 (d, 2H, J = 8.4 Hz, Ar), 7.27–7.36 (m, 5H, Bn) ppm. ^{13}C NMR ($CDCl_3$) 100 MHz: δ = 28.6 (CH_3, t-Bu), 38.9 (CH_2, $ArCH_2$), 51.3 (CH_3, CO_2Me), 51.7 (CH_2, NCH_2), 61.9 (CH, $CHCO_2Me$), 77.9 (C, t-Bu), 123.9 (CH, Ar), 126.8 (CH, Ar), 127.9 (CH, Ar), 128.1 (CH, Ar), 129.4 (CH, Ar), 132.0 (C, Ar), 139.3 (C, Ar), 153.9 (C, ArO), 174.8 (C, CO) ppm. ESI-MS (m/z): 342.1 ($M+H^+$); 364.2 ($M+Na^+$); 380.3 ($M+K^+$).

4.2.7. Methyl (2*S*)-2-(benzyl-(2-bromo-ethyl)-amino)-3-(4-*tert*-butoxy-phenyl)-propionate (8)

Neat 2-bromoethyl trifluoroethanesulfonate (892 mg, 3.47 mmol) was added into a solution of **7** (741 mg, 2.17 mmol) and 2,6-lutidine (784 μL, 6.73 mmol) stirring in anhydrous toluene (10 mL) at 0 °C. The resulting reaction mixture was stirred at rt for 24 h. More 2-bromo trifluoroethanesulfonate (300 mg, 1.17 mmol) was added and the reaction mixture was kept stirring for further 24 h, then diluted with EtOAc (20 mL) and washed with water (2 × 10 mL) and brine (2 × 10 mL). The organic layer was dried over Na_2SO_4, concentrated in vacuo and purified by column chromatography (petroleum ether/EtOAc 5:1–3:1) to give a colourless oil (372 mg, 38%). ^1H NMR ($CDCl_3$) 400 MHz: δ = 1.41 (s, 9H, t-Bu), 3.13–3.22 (m, 3H), 3.67 (t, 2H, J = 6.2 Hz, CH_2), 3.75 (s, 3H, CH_3), 3.74 (m, 1H, CHPh), 4.00 (d, 1H, J = 13.9 Hz , CHPh), 4.81 (t, 2H, J = 6.2 Hz, CH_2), 6.97 (d, 2H, J = 8.4 Hz, Ar), 7.09 (d, 2H, J = 8.4 Hz, Ar), 7.20–7.36 (m, 5H, Bn) ppm. ^{13}C NMR ($CDCl_3$) 100 MHz: δ = 26.2 (CH_2, CH_2Br), 28.8 (CH_3, t-Bu), 35.7 (CH_2, $ArCH_2$), 51.4 (CH_3, CO_2Me), 53.0 (CH_2, Bn), 64.9 (CH, $CHCO_2Me$), 74.4 (CH_2, CH_2N), 78.3 (C, t-Bu), 124.2 (CH, Ar), 127.3 (CH, Ar), 128.3 (CH, Ar), 128.6 (CH, Ar), 129.6 (CH, Ar), 132.8 (C, Ar), 139.0 (C, Ar), 153.9 (C, ArO), 172.9 (C, CO) ppm. ESI-MS (m/z): 448.1, 450.2 ($M+H^+$); 470.4, 472.0 ($M+H^+$).

4.2.8. Methyl (2*S*)-2-(benzyl-(2-((2-(bis-*tert*-butoxycarbonylmethyl-amino)-ethyl)-*tert*-butoxycarbonylmethyl-amino)-ethyl)-amino)-3-(4-*tert*-butoxy-phenyl)-propionate (10)

A suspension of **8** (372 mg, 0.830 mmol), tris-*tert*-butyl ethylenediaminotriacetate (**9**) (368 mg, 0.913 mmol) and Na_2CO_3 (264 mg, 2.49 mmol) in MeCN (3 mL) was heated under reflux for 36 h. The reaction mixture was diluted with EtOAc (15 mL), washed with water (2 × 5 mL) and brine (5 mL). The organic layer was dried over Na_2SO_4, concentrated in vacuo and purified by column chromatography (petroleum ether/EtOAc 5:1–3:1) to give a light-yellow oil (219 mg, 32%). ^1H NMR ($CDCl_3$) 400 MHz: δ = 1.31 (s, 9H, t-Bu), 1.38 (s, 27H, CO_2t-Bu), 2.71–2.91 (m, 10H, CH_2), 2.89 (dd, 1H, J = 14.0, 7.8 Hz, ArCH), 3.03 (dd, 1H, J = 14.0, 7.8 Hz, ArCH), 3.40 (s, 4H, CH_2CO_2t-Bu), 3.59 (d, 1H, J = 14.1 Hz, BnCH), 3.63 (s, 3H, CO_2Me), 3.65 (t, 1H, J = 7.8 Hz, NCH CO_2Me), 3.91 (d, 1H, J = 14.1 Hz, BnCH), 6.90 (d, 2H, J = 7.9 Hz, Ar), 7.01 (d, 2H, J = 7.9 Hz, Ar), 7.06–7.22 (m, 5H, Bn) ppm. ^{13}C NMR ($CDCl_3$) 100 MHz: δ = 28.1 (CH_3, t-Bu), 28.9 (CH_3, t-Bu), 35.3 (CH_2, $ArCH_2$), 51.2 (CH_3, CO_2Me), 51.6, 52.4, 52.6, 53.2, 55.9, 56.0, 56.2 (CH_2, NCH_2), 64.3 (CH, $CHCO_2Me$), 78.2 (C, t-Bu), 80.9 (C, t-Bu), 81.1 (C, t-Bu), 124.0 (CH, Ar), 127.0 (CH, Ar), 128.1 (CH, Ar), 128.7 (CH, Ar), 129.7 (CH, Ar), 133.1 (C, Ar), 139.3 (C, Ar), 153.7 (C, Ar), 170.5 (C, CO), 172.9 (C, CO) ppm. ESI-MS (m/z): 770.5 ($M+H^+$); 792.5 ($M+Na^+$).

4.2.9. (2*S*)-2-(2-((2-(Bis-carboxymethyl-amino)-ethyl)-carboxymethyl-amino)-ethylamino)-3-(4-hydroxy-phenyl)-propionic acid (L3)

A solution of **10** (160 mg, 0.208 mmol) and KOH (35.0 mg, 0.623 mmol), in 1:1 MeOH–H_2O (2 mL) was stirred at rt for 8 h. Then MeOH was removed in vacuo and the mixture was lyophilised after being acidified to pH 2. The resulting solid was triturated under acidic water (pH 2) and then suspended in $CHCl_3$ (2 mL) containing *i*-Pr_3SiH (5 μL) and treated with TFA (400 μL). The reaction mixture was stirred for 12 h and then concentrated in vacuo to give a white solid. The resulting solid was suspended in MeOH (5 mL) and treated with 10% Pd/C (25 mg); the reaction mixture was stirred under an atmosphere of H_2 for 18 h, then filtered over Celite and concentrated in vacuo to give a white solid. ^{1}H NMR (D_2O + NaOD, pD = 8.5) 400 MHz: δ = 2.44–3.01 (m, 10H), 3.35 (s, 6H), 3.80–4.03 (m, 1H), 6.68 (d, 2H, *J* = 8.3 Hz, Ar), 6.95 (d, 2H, *J* = 8.3 Hz, Ar) ppm. ^{13}C NMR (D_2O + NaOD) 100 MHz: δ = 37.2 (CH_2, $ArCH_2$), 46.5, 51.8, 52.5, 55.5, 58.3, 59.7 (CH_2, NCH_2), 65.3 (CH, $CHCO_2H$), 115.7 (CH, Ar), 129.3 (CH, Ar), 135.4 (C, Ar), 156.1 (C, ArOH), 176.3 (C, CO), 176.9 (C, CO) ppm. ESI-MS (*m*/*z*): 440.1 ($M-H^+$).

4.3. Incubation experiments

4.3.1. General incubation with tyrosinase

A solution of Mn(II) complex (Mn**L$_1$**, Mn**L$_2$** or Mn**L$_3$**) in 50 mM phosphate buffer at pH 6.5 (100 μL; 333 nmol) or in 5 mM hepes buffer at pH 7.4 (100 μL; 297 nmol) was treated with a solution of tyrosinase (10 μL; 50 U, 50 μL; 250 U or 100 μL; 500 U) in 50 mM phosphate buffer at pH 6.5 or in 5 mM hepes buffer at pH 7.4 and further diluted with the correspondent buffer, when necessary, to reach the final volume of 200 μL. The variation of the longitudinal water proton relaxation rate was followed over 20 h.

4.3.2. Cell culture

B16F10 melanoma cells (mouse) were obtained from American Type Culture Collection (ATCC, Manassas, USA), grown in Dulbecco's modified Eagle's medium (DMEM) containing 10% foetal bovine serum from Lonza (Lonza Sales AG, Verviers. Belgium), 100 U/mL penicillin and 100 mg/mL streptomycin and maintained at 310 K under 5% CO_2 conditions. After 3 days culture, the cells were harvested with trypsine/EDTA, counted with the Trypan-blue exclusion test, and assayed for tyrosinase activity.

4.3.3. Cellular tyrosinase activity assay

Ca. 1×10^6 B16F10 cells were washed with PBS, added to 0.5 mL of a 1 mM L-DOPA solution, sonicated to induce cell lysis and the absorbance at 475 nm was measured over time by maintaining the temperature of the reaction mixture at 37 °C. An extinction coefficient of 3700 M^{-1} cm^{-1} was used for the quantification of the DOPAchrome formation.

4.3.4. Mn**L$_2$** and Mn**L$_3$** incubation with B16-F10 homogenates

Ca. 5×10^6 cells were washed with PBS, harvested with trypsine/EDTA and added to a 1 mM solution of Mn**L$_2$** or Mn**L$_3$** in 5 mM hepes buffer at pH 7.4 (100 μL) and sonicated to induce cell lysis. The variation of the longitudinal water proton relaxation rate at 20 MHz was followed over time.

Acknowledgements

This work was supported by MIUR (PRIN 2007) and carried out under the frame of ESF COST Action D38. We thank Dr. Claudio Cassino for help with the measurement of the ESR spectra.

Supplementary data

Supplementary data associated with this article can be found, in the online version, at doi:10.1016/j.bmc.2010.07.064.

References and notes

1. Lauffer, R. B. *Chem. Rev.* **1987**, *87*, 901.
2. Caravan, P.; Ellison, J.; McMurry, T.; Lauffer, R. *Chem. Rev.* **1999**, *99*, 2293.
3. Tòth, E.; Helm, L.; Merbach, A. E. *Top. Curr. Chem.* **2002**, *221*, 61.
4. Aime, S.; Botta, M.; Terreno, E. *Adv. Inorg. Chem.* **2005**, *57*, 173.
5. Li, Y.; Huang, T. T.; Carlson, E. J.; Melov, S.; Ursell, P. C.; Olson, J. L.; Noble, L. J.; Yoshimura, M. P.; Berger, C.; Chan, P. H. *Nat. Genet.* **1995**, *11*, 376.
6. Wedler, F. C.; Denman, R. B. *Curr. Top. Cell Regul.* **1984**, *24*, 153.
7. Lim, K. O.; Stark, D. D.; Leese, P. T.; Pfefferbaum, A.; Rocklage, S. M.; Quay, S. C. *Radiology* **1991**, *178*, 79.
8. Kubicek, V.; Toth, E. *Adv. Inorg. Chem.* **2009**, *61*, 63.
9. Koretsky, A. P.; Silva, A. C. *NMR Biomed.* **2004**, *17*, 527.
10. Watanabe, T.; Natt, O.; Boretius, S.; Frahm, J.; Michaelis, T. *Magn. Reson. Med.* **2002**, *48*, 852.
11. Aoki, I.; Wu, Y. J.; Silva, A. C.; Lynch, R. M.; Koretsky, A. P. *Neuroimage* **2004**, *22*, 1046.
12. Pautler, R. G.; Silva, A. C.; Koretsky, A. P. *Magn. Reson. Med.* **1998**, *40*, 740.
13. Mankoff, D. A. *J. Nucl. Med.* **2007**, *48*, 18N.
14. Lowe, M. P. *Curr. Pharm. Biotechnol.* **2004**, *5*, 519.
15. Moats, R. A.; Fraser, S. E.; Meade, T. J. *Angew. Chem., Int. Ed.* **1997**, *36*, 726.
16. Giardiello, M.; Lowe, M. P.; Botta, M. *Chem. Commun.* **2007**, 4044.
17. Aime, S.; Geninatti Crich, S.; Gianolio, E.; Giovenzana, G. B.; Tei, L.; Terreno, E. *Coord. Chem. Rev.* **2006**, *250*, 1562.
18. Querol, M.; Bennett, D. G.; Sotak, C.; Kang, H. W.; Bogdanov, A., Jr. *ChemBioChem* **2007**, *8*, 1637.
19. Chen, J. W.; Pham, W.; Weissleder, R.; Bogdanov, A., Jr. *Magn. Reson. Med.* **2004**, *52*, 1021.
20. Aime, S.; Botta, M.; Milone, L.; Terreno, E. *Chem. Commun.* **1996**, 1265.
21. Aime, S.; Botta, M.; Gianolio, E.; Terreno, E. *Angew. Chem., Int. Ed.* **2000**, *39*, 747.
22. Aime, S.; Botta, M.; Fasano, M.; Terreno, E.; Kinchesh, P.; Calabi, L.; Paleari, L. *Magn. Reson. Med.* **1996**, *35*, 648.
23. Chen, J. W.; Pham, W.; Weissleder, R.; Bogdanov, A., Jr. *Mag. Reson. Med.* **2004**, *52*, 1021.
24. Jawaid, S.; Khan, T. H.; Osborn, H. M. I.; Williams, N. A. O. *Anticancer Agents Med. Chem.* **2009**, *9*, 717.
25. Williams, M. A.; Rapoport, H. *J. Org. Chem.* **1993**, *58*, 1151.
26. Chi, D. Y.; Kilbourn, M. R.; Katzenellenbogen, J. A.; Welch, M. J. *J. Org. Chem.* **1987**, *52*, 658.
27. Achilefu, S.; Wilhelm, R. R.; Jimenez, H. N.; Schmidt, M. A.; Srinivasan, A. *J. Org. Chem.* **2000**, *65*, 1562.
28. Crich, S. G.; Biancone, L.; Cantaluppi, V.; Esposito, D. D. G.; Russo, S.; Camussi, G.; Aime, S. *Magn. Reson. Med.* **2004**, *51*, 938.
29. Aime, S.; Anelli, P. L.; Botta, M.; Brocchetta, M.; Canton, S.; Fedeli, F.; Gianolio, E.; Terreno, E. *J. Biol. Inorg. Chem.* **2002**, *7*, 58.
30. Pawelek, J. M. *J. Invest. Dermatol.* **1976**, *66*, 201.
31. Petrescu, S. M.; Petrescu, A. J.; Titu, H. N.; Dwek, R. A.; Platt, F. M. *J. Biol. Chem.* **1997**, *272*, 15796.
32. Liu, S. H.; Pan, I. H.; Chu, I. M. *Biol. Pharm. Bull.* **2007**, *30*, 1135.
33. Tomita, Y.; Maeda, K.; Tagami, H. *Pigment Cell Res.* **1992**, *5*, 357.